The Effect of Adding ZrO_2 Nanoparticles to Fe-18Al-15Cr Alloys with Mechanical Alloying Process for Oxidation Resistance

Lolytah[1], Djoko Hadi Prajitno[2], Pawawoi[3]
{lolytah.hasri@gmail.com[1], dhppr@yahoo.co.id[2], pwawoitme92@gmail.com[3]}

Universitas Jenderal Achmad Yani[1], Badan Tenaga Nuklir Nasional[2],
Universitas Jenderal Achmad Yani[3]

Abstract. The purpose of this study is to make a compatible material for the application at high temperatures. Material that commonly used is superalloy but this material has low melting point. One material that can replace superalloy material for the application at high temperatures are intermetallic alloys and this alloys are very compatible to facing up Industrial Revolution 4.0. The intermetallic alloys have several characteristics such as high strength at high temperatures, high oxidation resistance, high melting points and low densities. The specimens are made at this research are intermetallic alloys of Fe-18Al-15Cr with variations in the addition of ZrO_2 nanoparticles (1%, 3% and 5%). The process of making specimens using one method of powder metallurgy. The process is Mechanical Alloying (MA) which aims to reduce the particle size, increase homogeneity and help to form new phases. In the high temperature oxidation process using a variable temperature at 800°C, 900°C and 1000°C for 4 hours. The result of metallographic testing showed the formation of the intermetallic phase Fe_3Al. The result of XRD testing showed the formation of oxide compounds on the surface of the specimen that are Cr_2O_3, Al_2O_3 and Fe_2O_3. Addition of small amount of ZrO_2 into the Fe-Al alloy is very effective to enhance the oxidation resistance and hardness of the material.

Keywords: Fe_3Al, Intermetallic, Mechanical Alloying, Oxidation, ZrO_2 Nanoparticles,

1 Introduction

In the aircraft industry, there is an Aero gas turbine engine that has a exhaust system that transmits turbine exhaust gases to the atmosphere at the speed, and in the direction needed, to provide the thrust produced. The design of the exhaust system has a considerable influence on jet engine performance. But, the exhaust system works if the combustion can works properly.

The combustion chamber has the difficult task of burning large quantities of fuel, supplied through the fuel spray nozzles, with extensive volumes of air, supplied by the compressor, and releasing the heat in such a manner that the air is expanded and accelerated to give a smooth stream of uniformly heated gas at all conditions required by the turbine. This task must be accomplished with the minimum loss in pressure and with the maximum heat release for the limited space available.

The amount of fuel added to the air will depend upon the temperature rise required. However, the maximum temperature is limited to within the range of 850 to 1700°C by the materials from which the turbine blades and nozzles are made [1].

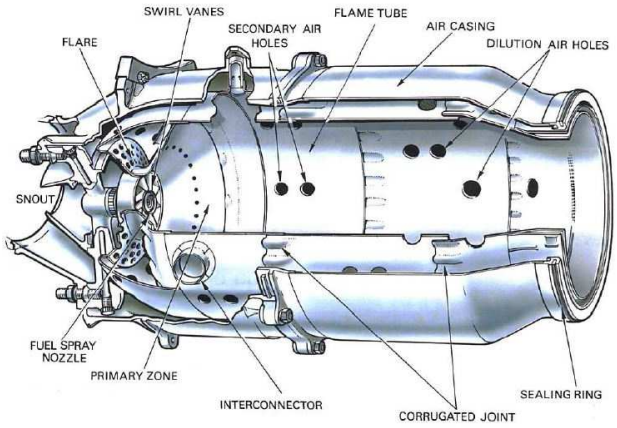

Fig. 1. An Early Combustion Chamber [1]

The air has already been heated to between 200 and 550°C by the work done during compression, giving a temperature rise requirement of 650 to 1150°C from the combustion process. Since the gas temperature required at the turbine varies with engine thrust, and in the case of the turbo-propeller engine upon the power required, the combustion chamber must also be capable of maintaining stable and efficient combustion over a wide range of engine operating conditions. Therefore, it is necessary to use materials and forms of construction that will withstand distortions and cracks, and prevent heat conduction in aircraft structures [1].

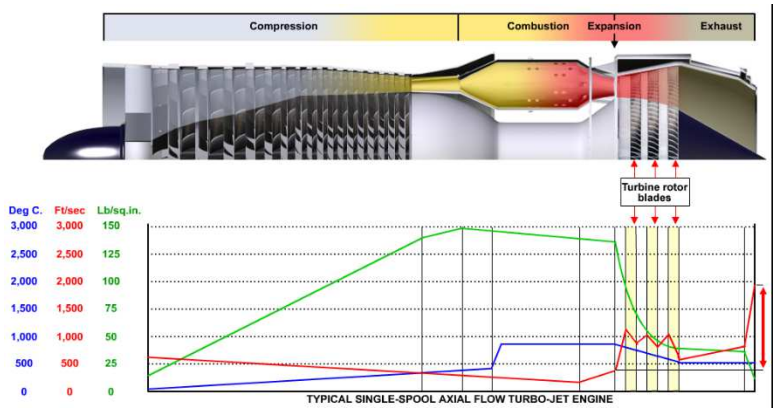

Fig. 2. Temperature, Axial Velocity and Total Pressure of Jet Engines [1]

The containing walls and internal parts of the combustion chamber must be capable of resisting the very high gas temperature in the primary zone. In practice, this is achieved by using the best heat resisting materials. The combustion chamber must also withstand corrosion due to the products of the combustion [1].

The purpose of this study is to make a compatible material for the application at high temperatures. High temperature material is a material that is able to maintain its properties or

does not decreasing it‘s quality at high temperatures and it‘s not easy to react with the surrounding environment at high operating temperatures.

The type of material commonly used in high temperature operating environments is super alloys. But this material has low melting point and it‘s quite expensive in terms of the material and the manufacturing process so that further research is carried out to produce a new type of material that is more efficient, the material is intermetallic alloy. Intermetallic alloys has high strength characteristics at high temperatures, high resistant oxidation and corrosion, high melting points and low density [2].

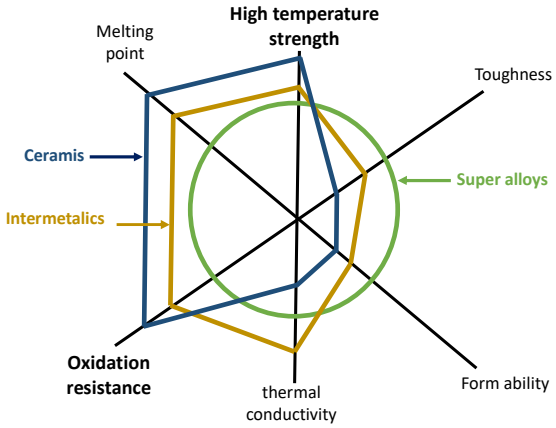

Fig. 3. Comparison of Three Materials (Super Alloys, Intermetallic and Ceramic) [2]

Intermetallic alloys that are good for use at high temperatures are iron-aluminum alloys (iron-aluminide) [3]. A material can be categorized as high temperature resistant if the material is able to operate without protection at a temperature of 600°C continuously. In iron and aluminum alloys, one of the phases formed is the Fe_3Al phase. The intermetallic alloy Fe_3Al is a things that make the material can operating at high temperatures. The advantages of using Fe-based are easy to get and cheap, low density, its durability increases with increasing temperature and has excellent oxidation resistance [4]. Fe_3Al-based intermetallic compounds are a very promising alloy group for alternative steel substitutes in high temperature applications and are open to future technology characterized with lower fuel consumption and reduce environmental impact [5].

Fe-based if combined with Al will produces intermetallic Fe-Al alloys especially Fe_3Al or FeAl. The Fe-Al alloy is good if used at high temperatures because it has oxidation resistance at high temperatures [6]. Fe_3Al intermetallic compounds showed unique physical properties and mechanical properties including high melting point (1540°C), high hardness (338 HV), low density (6,72 g/cc) and have a good oxidation and corrosion resistance. Fe_3Al retains the corrosion by forming a Al_2O_3 layer on the surface [7].

In the intermetallic compound Fe-Al-Cr, Fe as a base metal, Al as an alloy that increases toughness and tenacity and Cr (chromium) added to FeAl alloys can stabilizing the protective layer Al_2O_3 and increase the hardness, strength, toughness and oxidation resistance properties at high temperatures [2]. In addition ZrO_2 has many advantages as nano alloys. These advantages include having good corrosion resistance at temperatures above molten alumina

temperatures, stabilizing the protective layer of Al_2O_3, making a protective oxide thick layer formed at high temperatures, increase hardness and reducing porosity [8].

2 Experimental Procedure

Elemental Fe (>99%), Al (>95%), Cr (>99%), ZrO_2 (>99%) powders (Fe was supplied by MERCK, Al by MERCK, Cr by MERCK and ZrO_2 by Inframat Advanced Material). The alloy of this study had a chemical composition of 67Fe-18Al-15Cr + % ZrO_2 (1%, 3% and 5% ZrO_2) (otherwise stated the composition is in weight percent). To obtain chemical composition of the alloy, raw material proportion was set up as shown in Table 1, Table 2 and Table 3.

Table 1. Calculation of Material Balance (67Fe-18Al-15Cr + 1%ZrO_2)

Elements	%wt	Sample Vol (cm^3)	Elements Vol (cm^3)	ρ (g/cm^3)	Mass (gram)	5 pellets (gram)
Fe	67	0.285	0.191	7.860	1.501	7.505
Al	18	0.285	0.051	2.700	0.138	0.69
Cr	15	0.285	0.043	7.190	0.309	1.545
Element	%dopping	Sample Vol (cm^3)	Element Vol (cm^3)	ρ (g/cm^3)	Mass (gram)	5 pellets
ZrO2	1	0.285	0.003	5.680	0.017	0.085
			Mass of each sample =		1.965	9.825

Table 2. Calculation of **Material** Balance (67Fe-18Al-15Cr + 3%ZrO_2)

Elements	%wt	Sample Vol (cm^3)	Elements Vol (cm^3)	ρ (g/cm^3)	Mass (gram)	5 pellets (gram)
Fe	67	0.285	0.191	7.860	1.501	7.505
Al	18	0.285	0.051	2.700	0.138	0.69
Cr	15	0.285	0.043	7.190	0.309	1.545
Element	%dopping	Sample Vol (cm^3)	Element Vol (cm^3)	ρ (g/cm^3)	Mass (gram)	5 pellets
ZrO2	3	0.285	0.009	5.680	0.051	0.255
			Mass of each sample =		1.999	9.995

Table 3. Calculation of Material Balance (67Fe-18Al-15Cr + 5%ZrO_2)

Elements	%wt	Sample Vol (cm^3)	Elements Vol (cm^3)	ρ (g/cm^3)	Mass (gram)	5 pellets (gram)
Fe	67	0.285	0.191	7.860	1.501	7.505
Al	18	0.285	0.051	2.700	0.138	0.69
Cr	15	0.285	0.043	7.190	0.309	1.545
Element	%dopping	Sample Vol (cm^3)	Element Vol (cm^3)	ρ (g/cm^3)	Mass (gram)	5 pellets
ZrO2	5	0.285	0.014	5.680	0.080	0.4
			Mass of each sample =		2.028	10.14

The alloy of this study were milled in a planetary ball mill. The milling operation was performed at 1290 rpm for 3 hours. In all the experiments, nine hardened stainless steel balls with a diameter of 10 mm and twenty hardened stainless steel balls with a diameter of 5 mm were used with 9,8332 g powder mixture for alloy with 1% ZrO_2; 10,0073 g powder mixture for alloy with 3% ZrO_2 and 10,1761 g powder mixture for alloy with 5% ZrO_2 i.e. the ball-to-powder weight ratio was 10:1.

The powders milled for 3 hours were compacted by a load of 100 Kg/mm^2 to disks of 11 mm in diameter and 4,2 mm thickness. The milled powder was sintered in a sealed quartz tubes evacuated for 2 hours at 1000°C. Sintering was performed in a Tube Furnace. After sintering, the samples were cooled in the furnace to room temperature. Some samples are oxidized and some are not oxidized. Non-oxidized samples must be characterized early. Characterization that must be done consists of visual testing (measuring weight, height, diameter), microscopy testing by optical, phase and compound testing by XRD and hardness testing by Vickers.

Weighing and surface area measurement of each sample were carried out prior to oxidation test. Isothermal oxidation tests were carried out by heating the samples at 800, 900 dan 1000°C for 4 hours in a tube heat resistance electric furnace. After oxidation, the samples were cooled in the furnace to room temperature. Weighing of the oxidized samples was done to obtain the weight change of each sample. The samples after oxidation must be characterized by measuring height and diameter. Measuring the oxides thickness with an optical microscope was used to determine oxidation resistance at high temperatures and the samples were tested the hardness by indentation method using Zwick Hardness Vickers with a holding time of 10 seconds and the number of tests is 5 points.

To observe the microstructural changes during MA, the samples were polished to remove any surface contamination and then etched in HNA solution (3,3 mL CH_3COOH + 3,3 mL HNO_3 + 0,1 mL HF + 93,3 mL H_2O) with the immersion method for 5-8 seconds. Microstructure observation was carried out using an Olympus BX60M optical microscope with 1000x (20μm) magnification. The microstructural morphology of the compacted samples was characterized by SEM. The phase and compound testing after oxidation process was characterized by EDS.

Phase changes that occurred in the powders during milling and oxidation were investigated by X-ray diffraction using Philips Analytical PC-APD with a CuK_ radiation (_ = 0.1542 nm). The step size and step time were 0.05◦ and 1 s/step, respectively. The lattice parameter, long-range order parameter, crystallite size and lattice strain were calculated from the XRD data.

3 Results and Discussion

3.1 Visual testing, weight gain formula and weight gain data

Visual testing. Samples weight before and after oxidation is weighed and measurements the height and diameter from the samples using calipers and analytic balance.

Weight gain formula. Calculate the Δweight of the oxidation samples before calculating the weight gain with a formula like the following:

$$\Delta W = \text{weight after oxidation} - \text{weight before oxidation} = \text{gram} \quad (1)$$

After Δweight is obtained, calculate the surface area (Sa) of the samples with a formula like the following:

$$Sa = 2\Pi r(t+r) = mm^2 \quad (2)$$

After the two things above have been obtained, then the weight gain can be calculated by a formula like the following:

$$\text{Weight gain} = \frac{\Delta W}{Sa} = gr/mm^2 \quad (3)$$

Weight gain data. The following data are weight gain datas from oxidation samples that show weight before oxidation and weight after oxidation shown in **Table 4.**

Table 4. Dimension and Weight Observation Data Before and After Oxidation

%ZrO_2	Oxidation Temperature	Weight Before Oxidation (gram)	Weight After Oxidation (gram)	ΔW (gram)	Radius (r) mm	Height (t) mm	Surface Area mm²	Weight Gain gram/mm²
1		2.0925	2.1153	0.0228	5.5	4.2	335.038	0.0000680520
3	800°C	2.0986	2.1612	0.0626	5.5	4.2	335.038	0.0001868445
5		2.1442	2.1895	0.0453	5.5	4.2	335.038	0.0001352085
1		2.0886	2.1239	0.0353	5.5	4.2	335.038	0.0001053612
3	900°C	2.0451	2.1685	0.1234	5.5	4.2	335.038	0.0003683164
5		2.1340	2.1894	0.0554	5.5	4.2	335.038	0.0001653544
1		2.0671	2.1175	0.0504	5.5	4.2	335.038	0.0001504307
3	1000°C	2.0821	2.2345	0.1524	5.5	4.2	335.038	0.0004548738
5		2.1013	2.1645	0.0632	5.5	4.2	335.038	0.0001886353

From the table of data above, it shows that there is a change in weight, the weight increases after being oxidized. To clarify weight gain from all 9 samples, a weight gain curve was made:

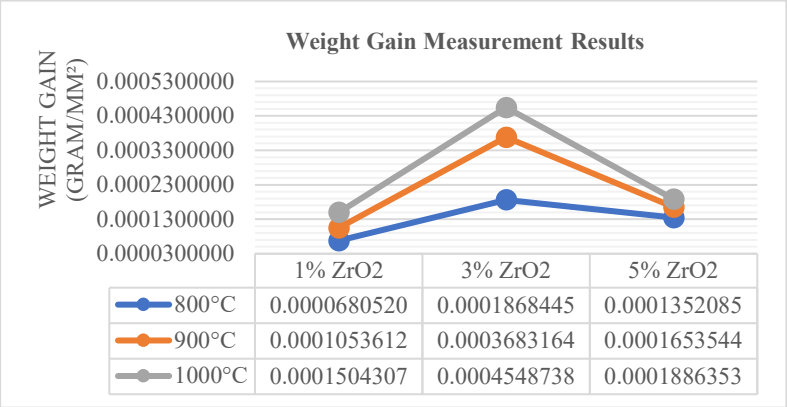

Fig. 4. Weight Gain Measurement Results Curve of All 9 Samples

3.2 Microstructure and phase formed

Microstructure. The figure below is a micro-structure of Fe-18Al-15Cr alloy which added ZrO_2 nanoparticles before and after oxidation with oxidation temperature according to the image below. Photographs of microstructure were carried out on the top surface of the sample for non-oxidized samples and in cross sections for oxidized samples.

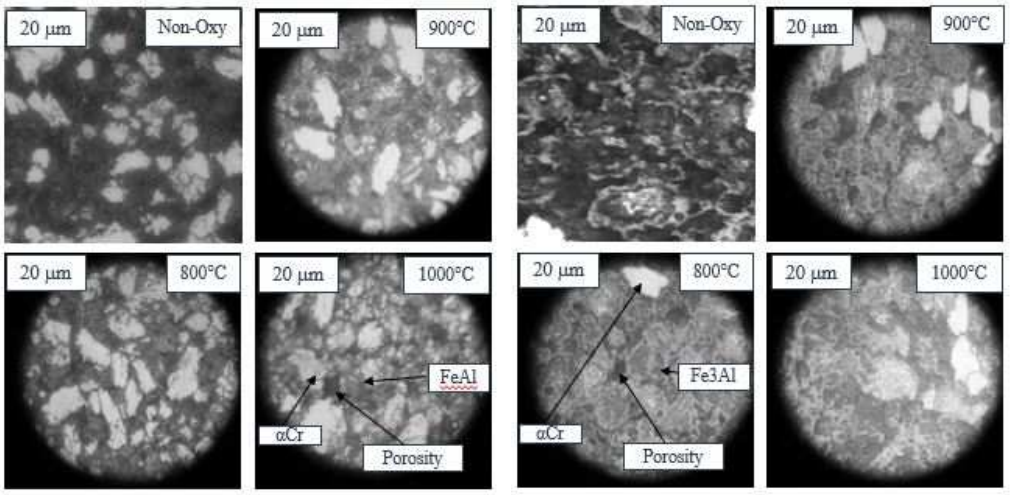

(a) (b)

Fig. 5. Microstructures of Fe-18Al-15Cr + 1% ZrO_2 Alloy (a) and Fe-18Al-15Cr + 3% ZrO_2 Alloy (b)

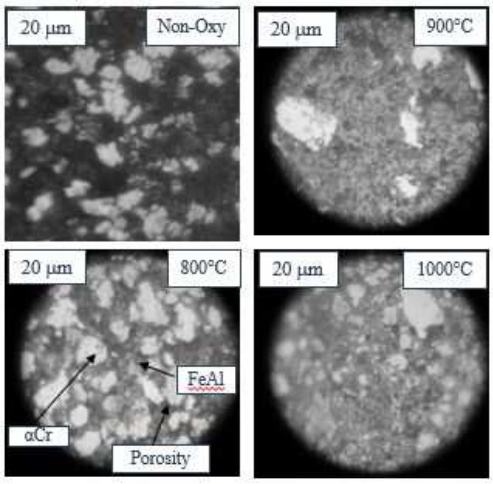

Fig. 6. Microstructures of Fe-18Al-15Cr + 5% ZrO_2 Alloy

Phase formed. The phase formed consists of αCr, FeAl and Fe_3Al and presence of porosity between phases. The shape of αCr in the micro structure is square and there is a round with white color and large in size. Porosity is marked in black color and it is located between grains. The FeAl and Fe_3Al phases are gray and their shape is like a cloud between αCr which is round white or square white [9]. In the 9 test samples with variations in oxidation temperature and the addition of ZrO_2 nanoparticles, the difference was in the form of grain changes in the microstructure. Oxidation temperature at 800^OC shows the sample has a fine grain shape but at a higher oxidation temperature, the grain size tends to more increase. Oxidation temperature at 1000^OC shows the sample has a coarse grains when adding just a little ZrO_2 nanoparticles that means the more ZrO_2 added will make the grains of microstructure more refined.

3.3 Hardness

Hardness. The Vickers hardness testing was carried out on 12 samples using 500 grams of load with diamond pyramid identor. Vickers hardness testing is carried out on the top surface of the sample for non-oxidized samples and on the cross section for oxidized samples. The following data are hardness testing results on 12 samples (Fe-18Al-15Cr + variation of $\%ZrO_2$) before and after oxidation process shown in Table 5.

Table 5. Hardness Vickers Number of All Samples

Sample	$\%ZrO_2$	Oxidation Temperature	Hardness (HVN)					
			1	2	3	4	5	Average
1	1		225.00	230.00	228.00	205.00	205.00	218.60
2	3	Non-Oxy	225.00	227.00	223.00	221.00	215.00	222.20
3	5		260.00	229.00	228.00	225.00	220.00	232.40
4	1		185.00	180.00	182.00	180.00	180.00	181.40
5	3	800°C	188.00	211.00	184.00	208.00	191.00	196.40
6	5		202.00	194.00	218.00	188.00	188.00	198.00
7	1		203.00	204.00	201.00	203.00	194.00	201.00
8	3	900°C	184.00	211.00	211.00	215.00	190.00	202.20
9	5		193.00	209.00	203.00	205.00	208.00	203.60
10	1		203.00	215.00	193.00	220.00	209.00	208.00
11	3	1000°C	220.00	201.00	201.00	215.00	215.00	210.40
12	5		215.00	218.00	229.00	215.00	203.00	216.00

Based on the data obtained from the table above, it can be seen that the effect of adding ZrO_2 nanoparticles to the alloy of Fe-18Al-15Cr powder has the highest average hardness value of 232.40 HVN. Hardness increases with increasing ZrO_2 as a dopping and increasing the oxidation temperature. This is analogous with the concept where in addition ZrO_2 has many advantages as nano alloys one of which is increasing the hardness number [8]. To clarify the hardness number from all 12 samples, a hardness results curve was made:

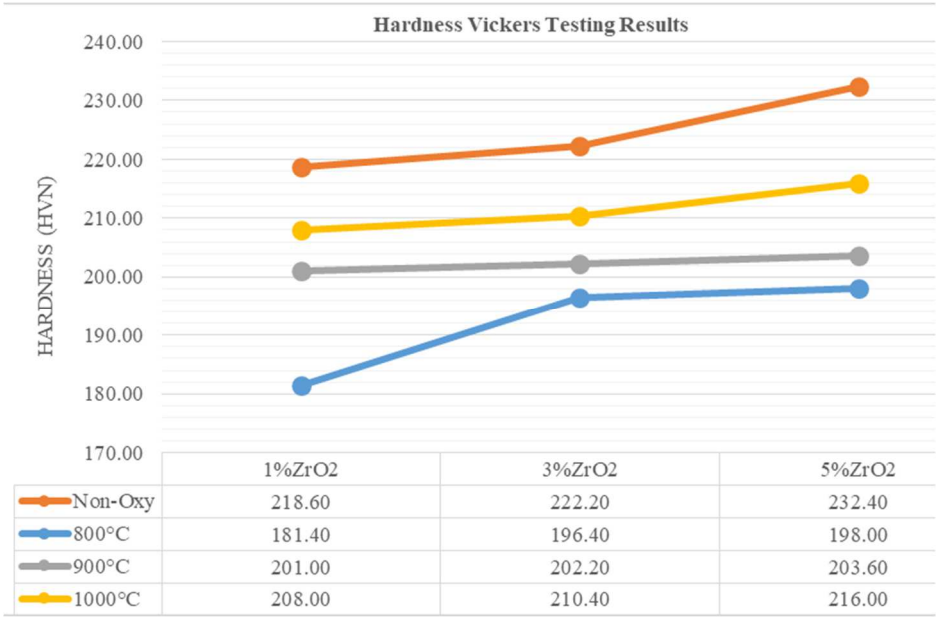

	1%ZrO2	3%ZrO2	5%ZrO2
Non-Oxy	218.60	222.20	232.40
800°C	181.40	196.40	198.00
900°C	201.00	202.20	203.60
1000°C	208.00	210.40	216.00

Fig. 7. Hardness Comparison Curve of Unoxidized and Oxidized Samples at 800°C, 900°C, 1000°C with Variations of ZrO_2 (1%, 3% and 5%)

3.4 Oxidation Thickness

Oxidation thickness. The figure below is a micro-structure of Fe-18Al-15Cr alloy which added ZrO_2 nanoparticles after oxidation with oxidation temperature according to the image below. Photographs of microstructure were carried out at cross sections.

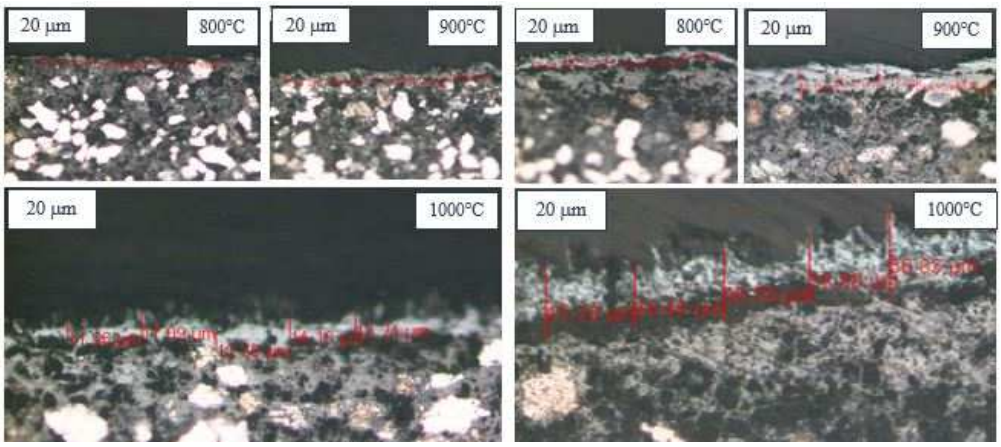

(a) (b)

Fig. 8. Oxidation Thickness of Fe-18Al-15Cr (a) adding 1% ZrO_2 (b) adding 3% ZrO_2

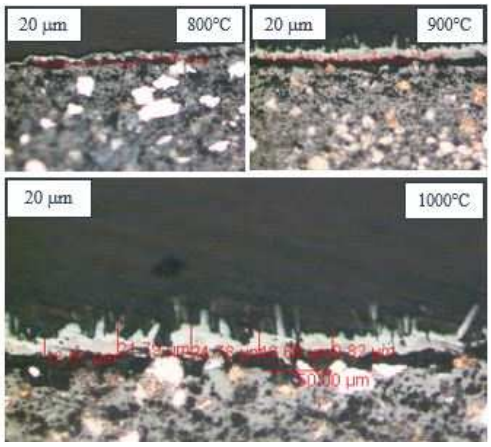

Fig. 9. Oxidation Thickness of Fe-18Al-15Cr + 5% ZrO_2 Alloy

The following data are oxide thickness measurement results on 9 samples (Fe-18Al-15Cr + variation of %ZrO_2) after oxidation process shown in Table 6.

Table 6. Oxide Thickness Measurement Data

Sample	%ZrO_2	Oxidation Temperature	Oxidation Thickness (µm)					
			1	2	3	4	5	Average
1	1		4.70	6.83	7.69	6.41	7.69	6.66
2	3	800°C	16.66	23.50	17.52	12.82	17.94	17.69
3	5		9.82	8.11	15.38	13.24	14.52	12.21
4	1		8.97	8.97	11.11	10.25	14.95	10.85
5	3	900°C	46.15	32.47	37.17	28.63	46.58	38.20
6	5		14.52	12.82	16.23	16.23	18.80	15.72
7	1		11.96	17.09	12.39	14.10	13.24	13.76
8	3	1000°C	45.29	38.46	46.58	38.88	56.83	45.21
9	5		13.67	21.79	24.78	16.66	9.82	17.34

Based on the data obtained from the table above, it can be seen that the effect of adding ZrO_2 nanoparticles to the alloy of Fe-18Al-15Cr powder has the highest average oxide thickness value of 45.21 µm. Oxides thickness increases with increasing the oxidation temperature. Oxide thickness can determine the oxidation resistance of a material where the thicker the oxide layer means the oxidation resistance of a material is low. From the data table above, it can be seen that the oxidation resistance of the material decreases when added ZrO2 nanoparticles as much as 3% but when added as much as 5% the oxidation resistance increases. This is because the addition of 3% ZrO_2 has not been effective against the oxidation resistance value of the material but will be very effective if the addition is as much as 5% ZrO_2 which will increase the oxidation resistance.

The oxidation thickness data obtained is proportional to the weight gain value after the oxidation process. This is analogous with the concept where the higher the weight gain value

the thicker the oxide thickness shown in Table 4. To clarify the oxidation thickness value from all 9 samples, a oxide thickness measurement results curve was made:

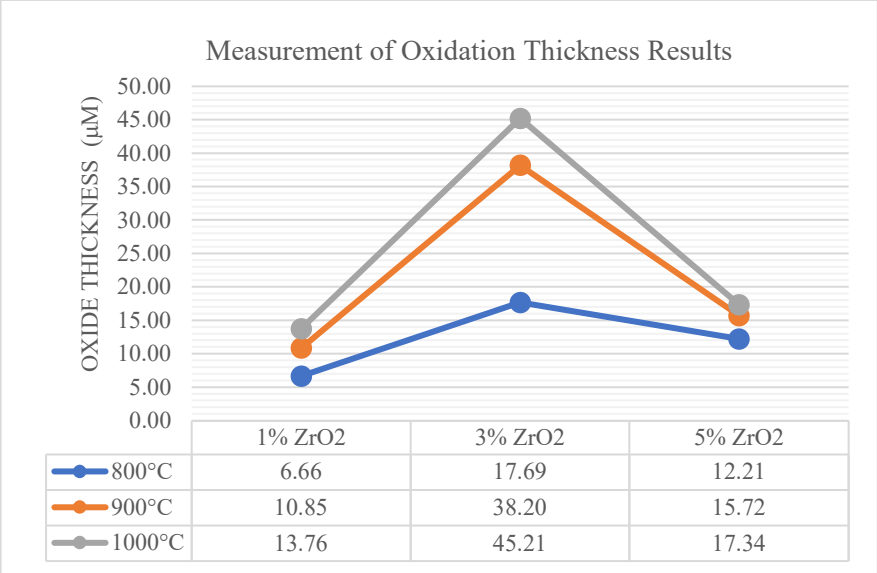

	1% ZrO2	3% ZrO2	5% ZrO2
800°C	6.66	17.69	12.21
900°C	10.85	38.20	15.72
1000°C	13.76	45.21	17.34

Fig. 10. Oxide Thickness Comparison Curve of Oxidized Samples at 800°C, 900°C, 1000°C with Variations of ZrO_2 (1%, 3% and 5%)

3.4 XRD and SEM-EDS Results

XRD. XRD testing was carried out on the surface of the sample to determine the compounds formed in Fe-18Al-15Cr + %ZrO_2 (1%, 3% and 5%) samples after oxidation which oxidation for 4 hours at 1000°C. The XRD analysis results, shown in Figure 11, confirmed that oxides of Fe_2O_3, Cr_2O_3 and Al_2O_3 were detected in all sample surfaces. It is believed that the outer parts of the scale was dominated by iron oxide of Fe_2O_3. Iron oxides such as Fe_2O_3 begin to form at temperatures around 570°C [3]. But the Fe_2O_3 oxide layer has properties not as a protective layer. Iron oxide of Fe_2O_3 is believed to be formed at the first stage of oxidation at all temperatures studied [10, 11], as the alloy rich in iron, even though these oxide are thermodynamically less stable compared with Al_2O_3 and Cr_2O_3. With time, underneath iron oxides depleted in Fe and consequently enrich the Al and Cr [10]. Enrichment of Cr in this region would drive formation of Cr_2O_3. However, Cr_2O_3 is less stable than Al_2O_3.Therefore, Al_2O_3 would form immediately bellow iron oxides scale [10]. Formation of this aluminium oxide reduced inward diffusion of oxygen to the alloy surface as the Fe^{n+} ions have larger size compared with other anions [11], making the outward diffusion of iron ions to the oxygen rich regions decrease. The growth of Al_2O_3 layer caused depletion aluminium content in the alloy below the scale [12]. Consequently, as the Cr content increased, Cr_2O_3 would form. Formation of reduces the possibility of iron oxides to form further [12]. Addition of Cr elements will increase oxidation resistance and ductility properties of Fe_3Al phase. In the formation of protective layer Cr_2O_3, Cr will play a role in reducing O_2 flux and reducing internal oxidation and accelerating the growth of Al_2O_3 layers under the Cr_2O_3 layer [11]. The scale mainly

consist out of Fe_2O_3, Cr_2O_3 and Al_2O_3 with small amounts of ZrO_2 scattered on the surface [13], this makes the position of the ZrO_2 peak in XRD patterns coincide with the major oxide layer Fe_2O_3.

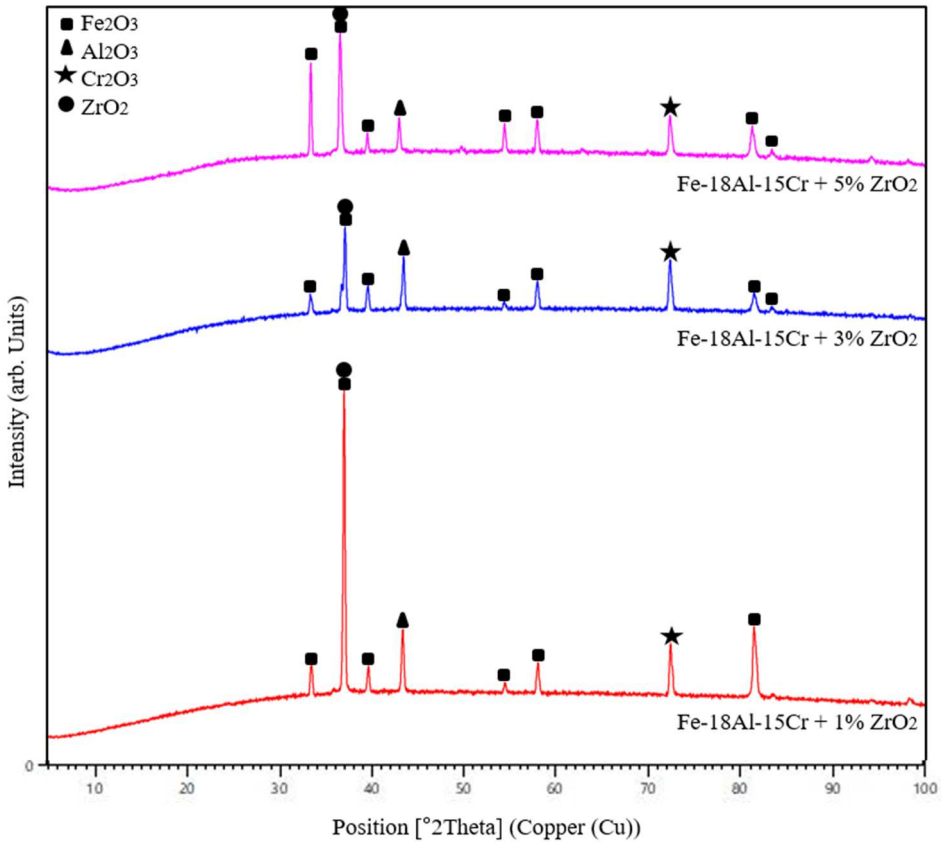

Fig. 11. XRD Patterns for Fe-18Al-15Cr + %ZrO_2 (1%, 3% and 5%) Oxidation at 1000°C for 4 Hours

SEM-EDS. SEM-EDS testing, shown in Figure 12-13, was carried out on the cross sections of the samples to determine percentage of Fe, Al, Cr, Zr and O elements in Fe-18Al-15Cr + %ZrO_2 (1% and 5%) samples after oxidation which oxidation at 900°C for 4 hours. EDS testing was carried out at the results of SEM micrograph with overall mapping to determine the percentage of the elements observation per position to see the distribution of elements to oxides and substrates of the samples, shown in Figure 14-15. The percentage of Zr in all points or positions has a stabil value according to the magnitude of the addition of ZrO_2 at the beginning of alloying. Al elements basically reacts with oxygen to form a protective layer of Al_2O_3 on the surface [7] while Cr (chromium) and ZrO_2 added to Fe Alloys can stabilize the protective layer Al_2O_3 [2, 8]. This is the reason why the percentage of oxygen is higher on the surface than in the middle of the sample because Al and Cr reacts with O_2 to produce a protective oxide layer on the surface. This also makes the percentage of Al and Cr higher on

the surface than in the middle of the sample. The things above make the Fe element on the surface of the sample less than in the middle of the sample.

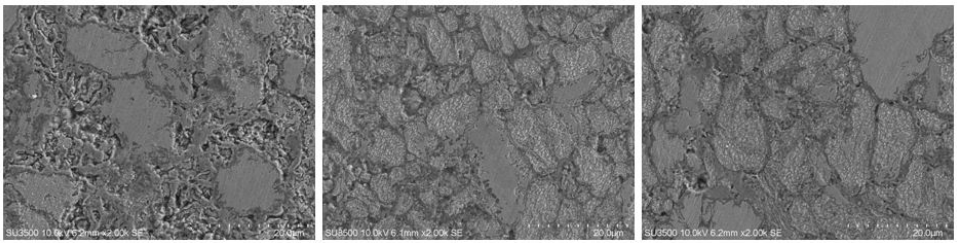

(1) (2) (3)

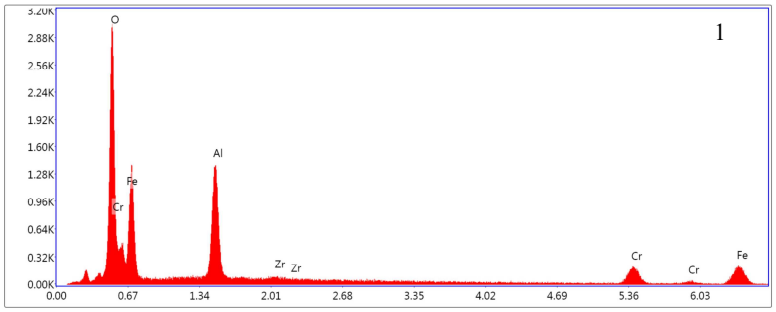

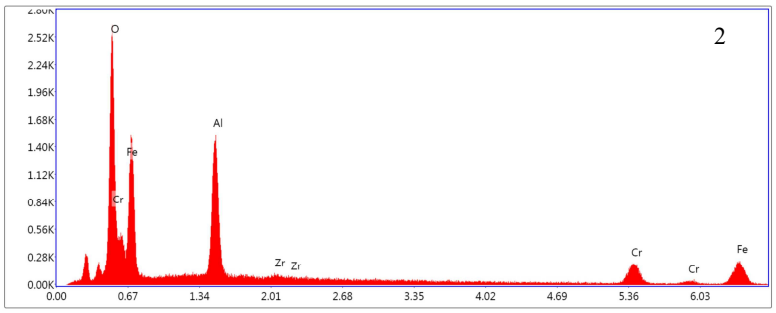

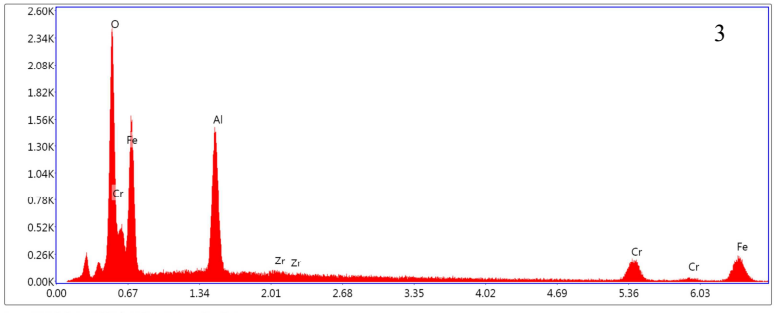

Fig. 12. SEM-EDS Micrograph For Fe-18Al-15Cr + 1% ZrO_2 Which Oxidation For 4 Hours At 900^0C With 2000x Magnification (Positions 1 To 3 Are From The Area Near The Surface To The Middle Of The Sample)

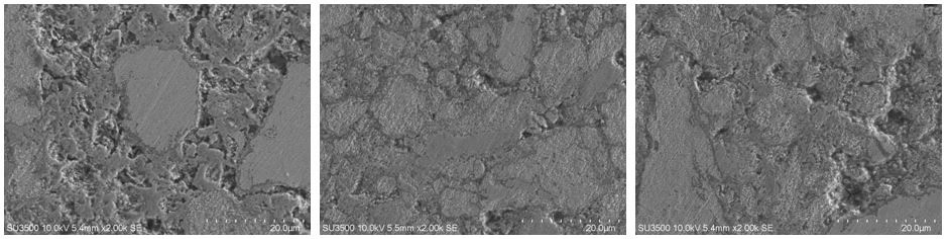

(1) (2) (3)

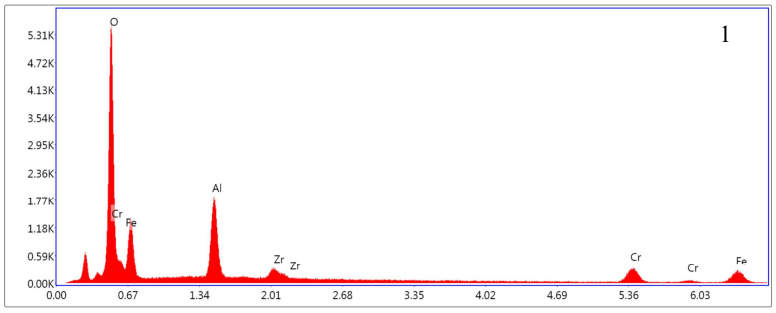

Lsec: 30.0 0 Cnts 0.000 keV Det: Octane Pro Det

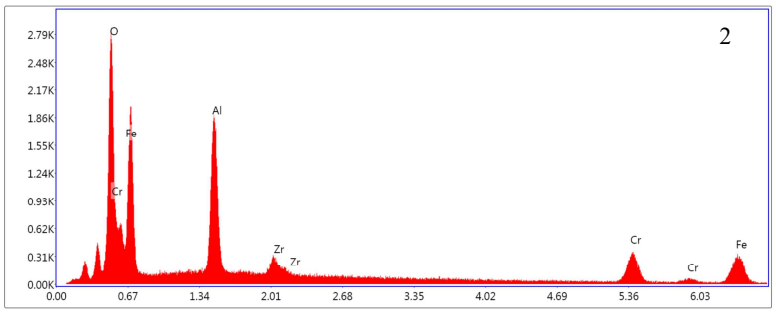

Lsec: 30.0 0 Cnts 0.000 keV Det: Octane Pro Det

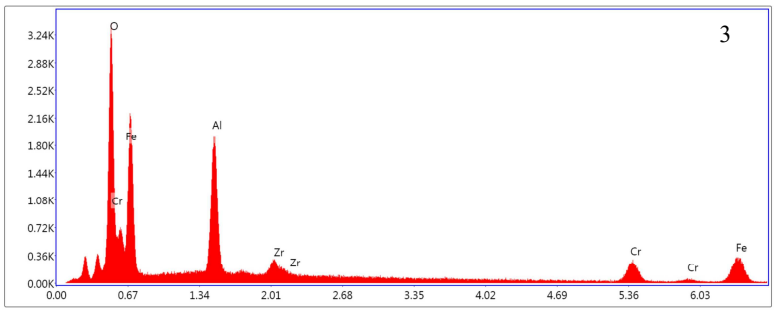

Lsec: 30.0 0 Cnts 0.000 keV Det: Octane Pro Det

Fig. 13. SEM-EDS Micrograph For Fe-18Al-15Cr + 5% ZrO_2 Which Oxidation For 4 Hours At 900^0C With 2000x Magnification (Positions 1 To 3 Are From The Area Near The Surface To The Middle Of The Sample)

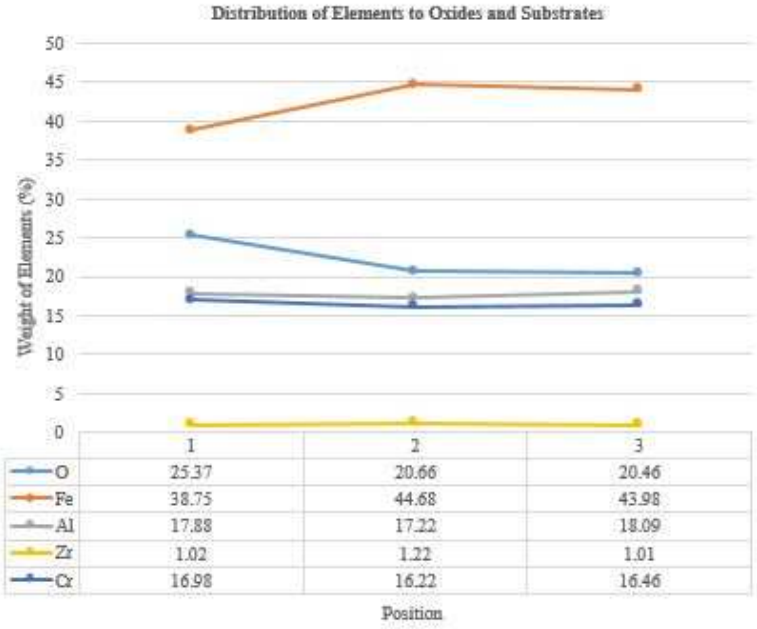

	1	2	3
O	25.37	20.66	20.46
Fe	38.75	44.68	43.98
Al	17.88	17.22	18.09
Zr	1.02	1.22	1.01
Cr	16.98	16.22	16.46

Fig. 14. Distribution Curve of Elements to Oxides and Substrates (Fe-18Al-15Cr + 1% ZrO_2 Oxidation at 900°C for 4 Hours)

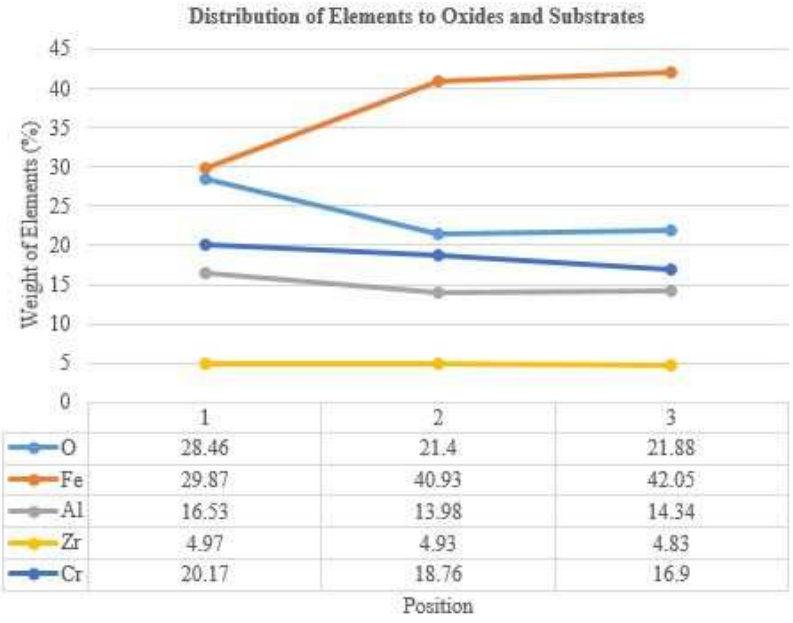

Fig. 15. Distribution Curve of Elements to Oxides and Substrates (Fe-18Al-15Cr + 5% ZrO_2 Oxidation at 900°C for 4 Hours)

4 Conclusion

The oxidation behaviour of Fe–18Al–15Cr + %ZrO_2 (1%, 3% and 5%) alloys designed for applications at high temperatures has been evaluated between 800, 900 and 1000°C. While all three alloys showed a very good oxidation resistance at 800°C, which compared favourably to those of other Fe_3Al-based alloys, they show increasing weight gains and oxide thickness at higher temperatures due to ingress of the oxidation into the sample. Scale formed on the surface of the samples consisted of oxides of Fe_2O_3, Al_2O_3 and Cr_2O_3 but dominated by Fe_2O_3. For the investigated alloys has beneficial effect from alloying the samples with 5 wt% ZrO_2. Addition of 3% ZrO_2 make a phenomenon of decreasing oxidation resistance that make the addition of ZrO_2 becomes ineffective. The addition of ZrO_2 made oxidation resistance increase when added 5% ZrO_2. Addition of small amount of ZrO_2 into the Fe-Al alloy has only insignificant effect on the mechanical properties, but it is worth to notice, that the addition of 5 wt% ZrO_2 is very effective to enhance the oxidation resistance and hardness of the material. Hardness increases with increasing oxidation temperature and %wt ZrO_2 as a doping. Oxide layer stability of Al2O3 is increased in Fe–18Al–15Cr + %wt ZrO_2 (1%, 3% and 5%) alloys. Because the compound element in the form of zirconium has dissolved in the Fe matrix. Non-oxidized samples have phase formed consists of αCr, FeAl and Fe_3Al and presence of porosity between phases. Fe_3Al intermetallic compounds showed unique physical properties and mechanical properties including high melting point and have a good oxidation and corrosion resistance [7] this is what makes it become a high temperature oxidation resistant material.

Acknowledgments

The authors gratefully acknowledge the support of National Nuclear Energy Agency of Indonesia (BATAN) and Degree Program of Metallurgical engineering, Jenderal Achmad Yani University Bandung Indonesia (UNJANI) for the research facilities. The first author would like to thank Mr Dr. Ir. Djoko Hadi Prajitno, MSME and Mr Pawawoi, ST. MT who supported the powders and for the help and valuable advice.

References

[1] Rolls Royce, "Rolls Royce - The Jet Engine," *The Jet Engine*. 1996.
[2] E. A. Basuki, *Paduan Logam Untuk Aplikasi Temperatur Tinggi Dan Penghematan Energi*. Bandung: ITB, 2016.
[3] G. S. Upadhyaya, "Powder Metallurgy Technology," *Cambridge Int. Sci. Publ.*, 2014, doi: 10.1073/pnas.0703993104.
[4] J. R. Davis, "ASM Specialty Handbook: Heat-Resistant Materials," in *ASM Specialty Handbook: Heat-Resistant Materials*, 1997.
[5] E. Airiskallio *et al.*, "High temperature oxidation of Fe-Al and Fe-Cr-Al alloys: The role of Cr as a chemically active element," *Corros. Sci.*, 2010, doi: 10.1016/j.corsci.2010.06.019.
[6] S. E. Haghighi, K. Janghorban, and S. Izadi, "Structural evolution of Fe-50 at.% Al powders during mechanical alloying and subsequent annealing processes," *J. Alloys Compd.*, 2010, doi: 10.1016/j.jallcom.2010.01.145.
[7] Z. B. Jiao, J. H. Luan, M. K. Miller, C. Y. Yu, and C. T. Liu, "Group precipitation and age hardening of nanostructured Fe-based alloys with ultra-high strengths," *Sci. Rep.*, 2016, doi: 10.1038/srep21364.
[8] J. M. A. Hotaťa, P.Kejzlara, M.Palmb, "The Effect of Zr on High-Temperature Oxidation Behaviour of Fe3Al-Based Alloys," *Corros. Sci.*, vol. 100, pp. 147–157, 2015, doi: 10.1016/j.corsci.2015.07.016.
[9] M. Mhadhbi, J. J. Suñolb, and M. Khitouni, "Influence of heat treatments on the structure of FeAl powders mixture obtained by mechanical alloying," in *Physics Procedia*, 2013, doi: 10.1016/j.phpro.2012.12.005.
[10] E. A. Basuki, D. C. Nababan, F. Muhammad, A. A. Korda, and D. H. Prajitno, "Isothermal Oxidation Behaviour of 69.5Fe-14Ni-9Al-7.5Cr Alloy at High Temperatures," *Int. J. Corros.*, 2019, doi: 10.1155/2019/8517648.
[11] P. Kofstad, *High Temperature Corrosion in Materials at High Temperatures Corrosion and Anti-Corrosives*. New York, USA: Elsevier Applied Science Publishers Ltd, 1988.
[12] N. K. Othman, N. Othman, J. Zhang, and D. J. Young, "Effects of water vapour on isothermal oxidation of chromia-forming alloys in Ar/O2 and Ar/H2 atmospheres," *Corros. Sci.*, 2009, doi: 10.1016/j.corsci.2009.08.032.
[13] A. Hotař, M. Palm, P. Kratochvíl, V. Vodičková, and S. Daniš, "High-temperature oxidation behaviour of Zr alloyed Fe 3Al-type iron aluminide," *Corros. Sci.*, 2012, doi: 10.1016/j.corsci.2012.05.027.